Fundamental Study on Glass Fiber-Reinforced Geopolymer Mortar

Chihiro Nagata[1], So Goto[2], Akihiro Maegawa[3], Takashi Hirose[4], Toshitsugu Inukai[5*]

[1]Advanced Course of Interdisciplinary Technology Development, National Institute of Technology, Gifu College, Gifu Prefecture, Japan

[2]Central Research Institute, Taiheiyo Cement Corporation, Chiba Prefecture, Japan

[3]Monozukuri Research Section, Mie Prefecture Industrial Research Institute, Mie Prefecture, Japan

[4]Design and Development Group, Maruji Concrete Industrial Co., Ltd, Gifu Prefecture, Japan

[5]Department of Architecture, National Institute of Technology, Gifu College, Gifu Prefecture, Japan

*Corresponding author: Toshitsugu Inukai, *inukai@gifu-nct.ac.jp*

Abstract

Glass fiber-reinforced mortars (GRM) are widely used exterior material in construction. However, their flexural strength decreases owing to the deterioration of glass fibers in alkali environment, which can be attributed to the formation of $Ca(OH)_2$. On the other hand, Geopolymers (GP) that do not use cement as a binder can hinder the formation of $Ca(OH)_2$. Therefore, it is assumed that GRM as a GP mortar can suppress the deterioration of alkali-resistant glass fibers. In this study, we experimentally examine the compression and flexural strength of glass fiber-reinforced GP mortar. Our results show that the compression strength of the GP mortar decreased as the addition rate of the retarding admixture increased, regardless of

the alkaline water or fly ash ratio. However, the fluidity enhanced with the addition of coagulation retardant with strength exceeding 1.0%. Furthermore, the glass fiber-reinforced GP mortar exhibited a relatively smaller flexural compared to glass fiber-reinforced mortars, using ordinary Portland or GRC cements. It was confirmed that there was no alkali-induced deterioration of the alkali-resistant glass fiber until 28 d of material age.

1. Introduction

Exterior materials for construction have excellent earthquake and fire resistance, are lightweight, and have high heat insulation. Glass fiber-reinforced mortar (GRM), which uses alkali-resistant glass fibers (ARG), is a widely used exterior construction material. GRM are manufactured from non-combustible materials and have large flexural strengths. The thin cross-sectional design enables fabricating lightweight components. However, the flexural strength of GRM decreases as the material ages, owing to glass fiber deterioration in alkaline environments such as cement [1]. This can be attributed to the $Ca(OH)_2$ produced during the hydration of cement. The progression of major alkali-induced deterioration cannot be avoided, even with ARG. Therefore, GRM generally uses GRC cement to inhibit the generation of $Ca(OH)_2$ hydration and hardening of cement [1].

Geopolymers (GP) that do not use cement as a binder have been proposed previously [2, 3]. GP can use fly ash (FA) generated from coal-fired power plants as an active filler, effectively reducing CO_2 emissions and promoting efficient reuse of industrial by-products. Furthermore, GP hardens cement via polycondensation reactions between alumina silica powder (active filler) and an alkaline solution, which does not produce $Ca(OH)_2$ during the reaction, unlike the hydration reaction of cement [4]. Therefore, it can be inferred that using GRM as a GP mortar may suppress the progress of ARG deterioration.

Glass fiber-reinforced geopolymers (GRGP) [5, 6] have attracted significant research interest. However, ARG deterioration [6] has not been investigated thoroughly. It is essential to evaluate the durability of GRGP, which uses a high-concentration alkaline solution, against

ARG deterioration from the initial stages of material age. It is also necessary to realize flexural strengths greater than 10 N/mm2 to meet the material standards [7] for GRC plates.

Therefore, in this study, we examined the compression and flexural strength of GRGP to improve its durability (suppression of ARG deterioration). First, to determine the mix proportion of GRGP, we examined (Experiment 1) how the alkaline water / fly ash ratio (AW/F) and retarding admixture (ST) addition rate affect the compression strength and flow of ARG-free GP mortar over time. In two subsequent experiments (Experiments 1 and 2), we examined how addition of ARG affected the compression and flexural strength of GRGP.

2. Effects of mix proportion design conditions on the changes in GP mortar compression strength and flow values over time (Experiment 1)

2.1. Outline of the experiment

2.1.1. Experimental factors

The experimental factors (AW/F and the ST addition rate) are shown in Table 1.

2.1.2. Materials and mix proportion used

Table 2 shows the materials used, and Table 3 shows the X-ray analysis results of FA after finely pulverizing JIS Class II FA (FAII) to approximately 7000 cm^2/g (FAII7). The chemical composition of the materials used was measured with a fluorescent X-ray analyzer. Crystalline minerals (quartz and mullite) were quantified from the calibration curve prepared using a powder X-ray diffractometer, and the residue was calculated as an amorphous phase.

Figure 1 shows the particle size distribution of FAII7. The particle size distribution of FAII is also shown for comparison. It can be seen from the figure that the FAII7 particles have smaller distribution width of the relative
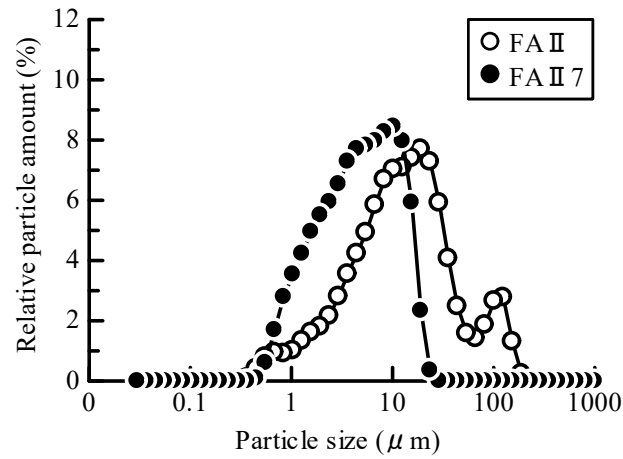
Table 1. Experimental factors (Experiment 1)

Factors	Levels
AW/F(%)	42, 46, 50
Extra addition ratio of ST to F (%)	0, 1.0, 2.0, 3.0

Table 2. Materials used (Experiments 1-3)

Material names	Marks	Types	Physical properties
Fly ash	F	A power plant Fly ash JIS type II Fine grinding: Presence	Blaine (cm^2/g) : 7822 Density (g/cm^3) : 2.45
Cement	OPC	Ordinary portland cement	Blaine (cm^2/g) : 3480, Density (g/cm^3) : 3.16
	GRC	GRC cement	Blaine (cm^2/g) : 4690, Density (g/cm^3) : 2.97
Fine aggregate	S	Dry Silica Sand (No.7)	Absolute dry density (g/cm^3) : 2.68
water	W	Tap water	-
Alkaline additives	NS	Sodium metasilicate	Density (g/cm^3) : 2.61
Setting retarder	ST	Anhydrous citric acid ($C_6H_8O_7$)	Density (g/cm^3) : 1.66
Alkali resistant glass fiber	ARG	Chopped strand	Strand : About 100 filaments of 18 μm are bundled. Fiber length (mm) : 19, 25
Chemical admixture	AD	High-range AE water reducing agent standard type I	Main component : Polycarboxylic-acid copolymer
		Water reducing agent type I	Main component : Alkyl allyl sulfonate high condensate

Table 3. X-ray analysis results of FAII7 (Experiments 1-3)

(%)

FA type	Chemical compositions						Glass phase amount
	SiO_2	Al_2O_3	Fe_2O_3	CaO	MgO	Ig.loss	
FA II 7	64.8	20.7	4.2	2.2	1.2	3.3	59.7

Figure 1. FA particle size distribution (Experiments 1-3)

particle amount and particle diameter, compared to the FAII particles.

Table 4 shows the mix proportion of the GP mortar. The AW in Table 4 indicates W + NS, and the design air volume is set to 2%. A mix proportion with the highest measured compression strength reported previously [2] was used as a reference for the amount of added NS, and the concentration of the aqueous NS solution was set to 3.0 mol/L.

2.1.3. Mixing and flow tests

The mixing was conducted using the method shown in Figure 2, using experimental results reported previously [3]. Mixing could not be achieved for the mixing time shown in the figure for an AW/F of 42%, and thus mixing was extended at a slow speed for 60 s and at a high speed for 120 s After the specified mixing time ended.

Table 4. GP mortar mix proportion (Experiment 1)

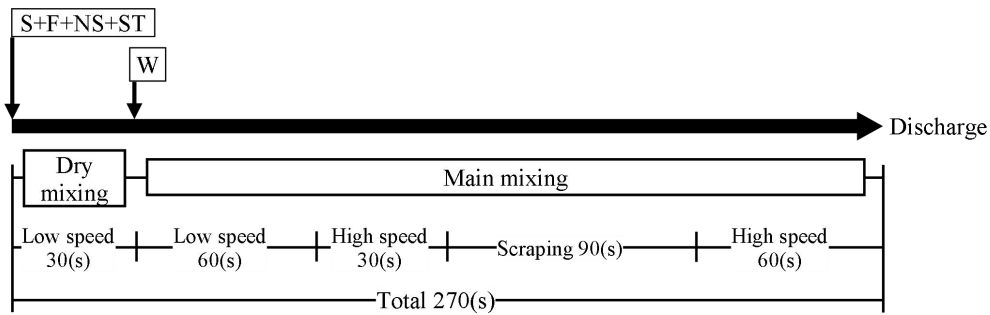| NS added amount*)	AW/F (%)	ST addition ratio (%)	Air (%)	S/F	Unit weight (kg/m^3)				Weight (kg)
					F	AW		S	
						W	NS		ST
3.0	42	0	2	0.6	-	-	-	-	-
		1.0			1006	296	127	604	10.1
		2.0			1006	296	127	604	20.1
		3.0			1006	296	127	604	30,1
	46	0			973	314	134	584	-
		1.0			973	314	134	584	9.7
		2.0			973	314	134	584	19.5
		3.0			973	314	134	584	29.2
	50	0			942	330	141	565	-
		1.0			942	330	141	565	9.4
		2.0			942	330	141	565	18.8
		3.0			942	330	141	565	28.3

*)Converted to NSaq concentration (mol/L)

Figure 2. GP mortar mixing method (Experiment 1)

Flow experiments were conducted according to the JIS R 5201, "Physical Testing Methods for Cement." Furthermore, the flow values over time were measured after mixing the sample for 30 s, immediately before starting the measurements. The rate of decrease in the flow rate was calculated using Eq. (1).

$$FL_d = (FL_s - FL_t) / FL_s \times 100 \tag{1}$$

FL_d: rate of decrease of the flow rate (%)

FL_s: flow rate immediately after the end of mixing

FL_t: flow rate t hours after the end of mixing

2.1.4. Compression strength tests

The compression strength test was conducted according to the JIS A 1142, "Method of Test for Fine Aggregate Containing Organic Impurities by Compressive Strength of Mortar." The specimen dimensions were set as φ = 50×100 mm, and the sample was divided into two layers; each layer compacted with a table vibrator for 30 s. The specimen was sealed and cured at 20 °C in a mold with the upper surface wrapped until reaching a material age of 28 d.

2.2. Experimental results and discussion

Table 5 shows the results of the flow value measurement. Mixing could not be carried out for specimens with AW/F of 42% and ST addition rate of 0%. It can be seen in Table 5 that the flow value increased with the AW/F.

Table 5. Flow value measurement results (Experiment 1)

AW/F (%)	Flow			
	ST addition ratio (%)			
	0	1.0	2.0	3.0
42	-	173.6	178.4	181.4
46	217.4	230.7	239.7	235.5
50	256.2	254.8	260.4	261.7

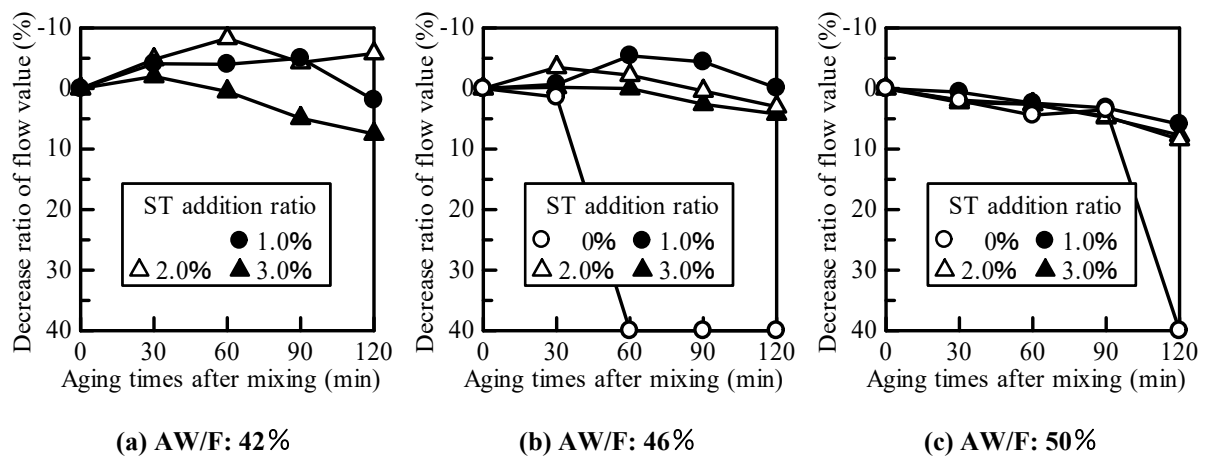(a) AW/F: 42%   (b) AW/F: 46%   (c) AW/F: 50%

Figure 3. Relationship between rate of decrease of flow value and time elapsed since the end of mixing (Experiment 1)
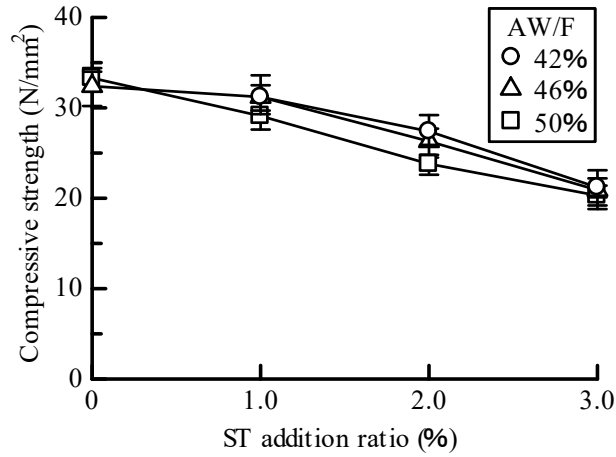
Figure 4. Relationship between compression strength and ST addition rate (Experiment 1)

Moreover, ST addition rate did not affect the flow value at any AW/F.

Figure 3 shows the relationship between the rate of decrease of the flow rate and with time after mixing ended. The rate of decrease of the flow rate was uniformly set to 40%, as shown in the figure, when the fluidity decreased and it was not possible to measure the flow value. It can be seen at all AW/F levels that the rate of decrease of the flow rate reduced upon adding ST, and measurements could not be carried out within 120 min when ST was not added. Moreover, no differences were noticed due to the ST addition rate in the rate of decrease in the flow rate, and the decrease in the fluidity improved upon adding ST with a strength greater than 1.0%.

Figure 4 shows the relationship between the compression strength and the ST addition rate. It can be seen at all AW/F levels that the compression strength decreased when the ST addition rate increased. Moreover, it can be seen that the compression strength increased with AW/F. These results are consistent with previous measurements [8], where the compression strength increased when the amount of water/GP solid matter decreased.

Thus, the AW/F needs to be kept small, and the ST strength should be greater than 1.0%, to maintain fluidity of the GP mortar and maximize the compression strength. Therefore, we conducted Experiments 2 and 3 with a mix proportion where the AW/F was set to 42% and the ST addition rate was set to 1.0%.

3. Effect of adding ARG on GRGP the compression and flexural strengths (Experiments 2 and 3)

3.1. Compression strength (Experiment 2)

3.1.1. Outline of the experiment

3.1.1.1. Experimental factors

Table 6 lists the experimental factors. The ARG fiber length, material age, and curing method were set as the experimental factors. The GRC cement used in Experiment 3 requires the curing conditions shown in Figure 5; therefore, the heating and curing conditions used in all specimens were set as equivalent. The specimens underwent two hours of pre-curing, after which they were sealed and cured at 20 °C after heating and curing until the specified material age. For heating and curing, a specimen mold filled with samples was placed within a container box filled with water so that the interior was moist. Sealing and curing were performed in the same manner as in Experiment 1.

Table 6. Experimental factors (Experiment 2)

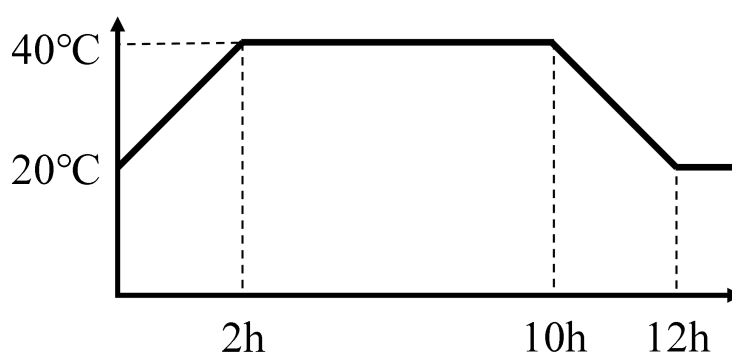| Factors	Levels
ARG fiber length (mm)	19, 25
Curing age (days)	1, 7, 28
Curing method	Sealed, Heat

Figure 5. Heating and curing conditions (Experiments 2 and 3)

Table 7. Experimental factors (Experiment 2)

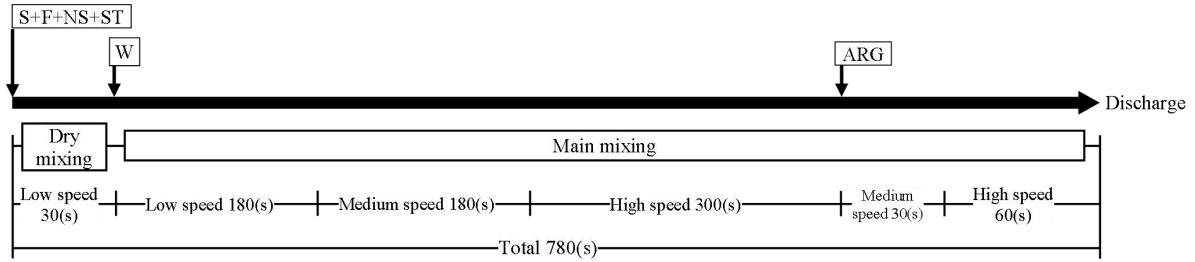| NS added amount*)	AW/F (%)	ST addition ratio (%)	ARG mixing ratio (%)	ARG fiber length (mm)	Air (%)	S/F	Unit weight (kg/m³)				Weight (kg)	
							F	AW		S	ST	ARG
								W	NS			
3.0	42	1.0	0	-	2	0.6	1006	296	127	604	10.1	-
			2.0	19			1006	296	127	604	10.1	40.7
				25			1006	296	127	604	10.1	40.7

*)Converted to NSaq concentration (mol/L)

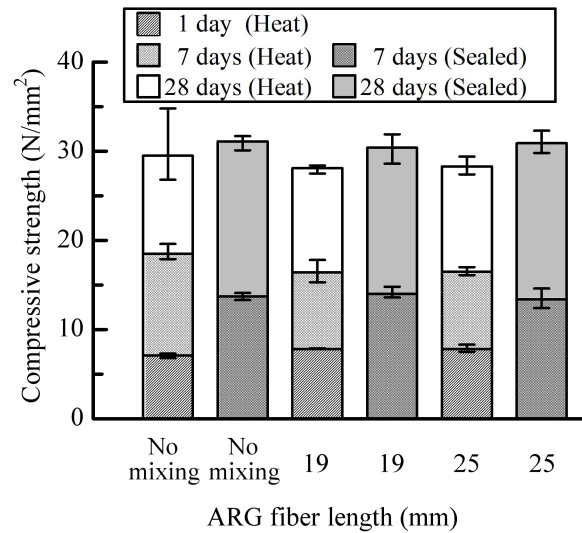**Figure 6. GRGP mixing method (Experiments 2 and 3)**

Figure 7. Relationship between compression strength and ARG fiber length (Experiment 2)

3.1.1.2. Materials and mix proportion used

The materials used were the same as those used in Experiment 1 (see Table 2), and the GRGP mix proportion are shown in Table 7.

3.1.1.3.   Mixing

Mixing was conducted as in a previous report [7], in addition to the method shown in Figure 6 with an omni-mixer.

3.1.1.4.   Compression strength tests

The compression strength test was carried out in the same manner as in Experiment 1.

3.1.2. Experimental results and discussion

The relationship between the compression strength and ARG fiber length is shown in Figure 7. It was not possible to remove the mold at a material age of 1 d during sealing and curing, and the results are shown only for material ages of 7 and 28 d. It can be seen in the figure that the heating and curing methods yielded higher initial strength and smaller strength at 28 d, compared to the sealing and curing methods. Moreover, no differences were noticed in the compression strength with changes in the ARG fiber length, regardless of the curing method used. These results are different from previously reported results [5], where increases in the glass fiber mixing rate tended to increase the compression strength. However, it has been shown previously [9] that the fiber orientation direction had a large effect on the compression strength, with compression strength increasing or decreasing when loads were applied orthogonally or parallel to the fibers. We oriented samples randomly in the experiments, and thus it is assumed that ARG mixing does not influence the compression strength.

3.2. Flexural strength (Experiment 3)

3.2.1. Outline of the experiment

3.2.1.1. Experimental factors

Table 8 shows the experimental factors. GRM specimens using OPC and GRC cement were used to compare the flexural strength.

3.2.1.2. Materials and mix proportion used

The materials used were the same as those used in Experiment 1 (see Table 2), and the GRM mix proportion are shown in Table 9. The GRM mix proportion was set with a W/C of 35% and an S/C of 0.6, assuming that it would be used as an exterior material for construction [10]. The GRGP mix proportion was set as that in Experiment 2.

3.2.1.3. Mixing and flow tests

GRM mixing was conducted using the method shown in Figure 8. GRGP mixing was conducted in the same way as in Experiment 2.

Using the method in reference [10], flow test measurements were carried out for the mortar flow value before and after adding (natural flow value) and mixing ARG (tapping flow value). The natural flow value was measured using a natural flow cone (PVC, φ 55×50 mm), and the tapping flow value was measured using a flow cone similar to that in Experiment 1. The target flow value of the GRM was set to a natural flow value of 120 – 190 mm, based on reference [10].

3.2.1.4. *Flexural strength tests*

The flexural strength test used a three-point flexural load with a span of 120 mm according to the JCI-S-002-2003, "Method of Test for Load Displacement Curve of Fiber-Reinforced concrete using a notched beam." The specimen dimensions were set as 40×40×160 mm, and three specimens were prepared for each condition. Only the curing method was used in this experiment.

Table 8. Experimental factors (Experiment 3)

Factors	Levels
ARG fiber length (mm)	19, 25
Curing age (days)	1, 7, 28

Table 9. GRM mix proportion (Experiment 3)

Cement types	W/C (%)	ARG mixing ratio (%)	ARG fiber length (mm)	Air*) (%)	S/C	Unit weight (kg/m3)				Weight (kg)	
						C	W	S	AD	ST	ARG
OPC	35	0	-	0	0.6	1123	393	674	19.1	-	-
		2.0	19			1123	393	674	19.1	-	43.8
			25			1123	393	674	19.1	-	43.8
GRC		0	-			1098	384	659	22.0	4.4	-
		2.0	19			1098	384	659	22.0	4.4	42.8
			25			1098	384	659	22.0	4.4	42.8

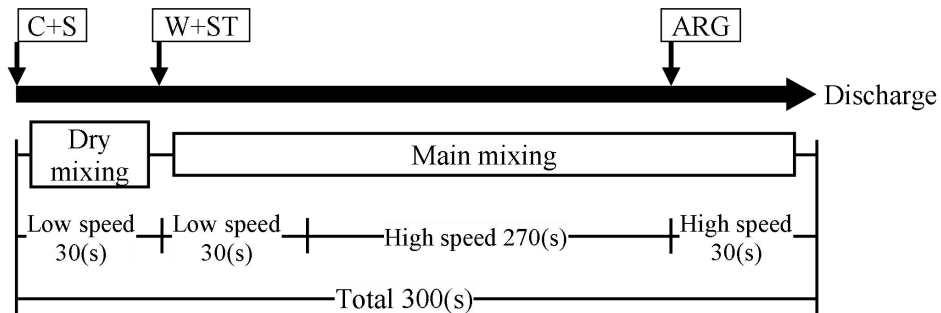*)Air was set to 0% in mixing calculation

Figure 8. GRM mixing method (Experiment 3)

Table 10. Flow value measurement results (Experiment 3)

ARG fiber length (mm)	ARG no mixing flow			ARG mixing flow		
	OPC	GRC	GP	OPC	GRC	GP
0	145	168	109	-	-	-
19	137	170	103	230	265	154
25	156	174	106	199	230	147

(a) ARG No Mixing   (b) ARG Fiber Length:19mm   (c) ARG Fiber Length:25mm

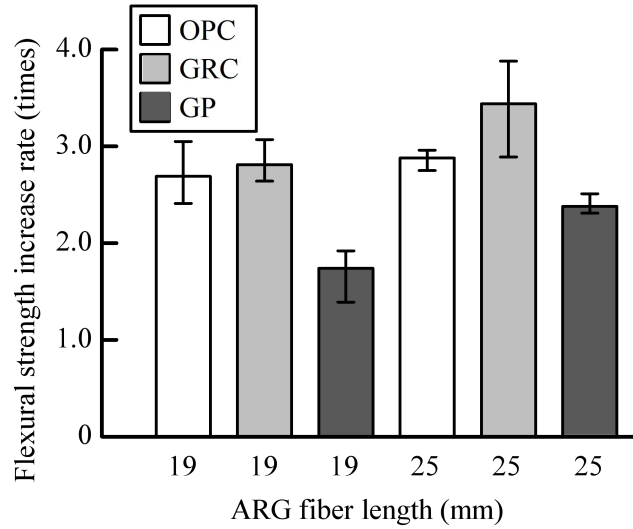**Figure 9. Relationship between flexural strength and material age (Experiment 3)**

Figure 10. Relationship between factor of flexural strength increase and ARG fiber length (Experiment 3)

3.2.2. Experimental results and discussion

Table 10 shows the flow value measurement results. It can be seen from the table that longer ARG fiber lengths decreased the tapping flow value.

Figure 9 shows the relationship between the flexural strength and material age. The flexural strength was set as the value at the time of maximum load. It can be seen from the figure that longer ARG fiber lengths tended to increase the flexural strength, but there were no differences due to fiber length in the flexural strength of OPC at a material age of 28 d. It is not clear why the flexural strength decreased at a material age of 28 d, but it has been reported previously that there were no differences in flexural strength between materials with fiber lengths of 19 or 25 mm at a material age of 28 d [11]. The flexural strength also increased in the order of GRC, OPC, and GP, regardless of the ARG fiber length. The reason why the flexural strength of GRCP was the smallest was because water reducing agents cannot be used as with OPC to reduce AW/F, and the maximum temperature of the heating and curing for GP is low, when the matrix mortar strength decreases.

Figure 10 shows the relationship between the increase in flexural strength and the ARG fiber length. The factor of flexural strength increase was defined as the ratio of the flexural strength when ARG was added at a material age of 28 d and the flexural strength without ARG added. It can be seen from the figure that longer ARG fiber lengths increased the flexural strength factor. The flexural strength increases also increased in the order of GRC, OPC, and GP, regardless of the ARG fiber length. This may be attributed to the fact that GP without ARG had a flexural strength 50 - 65% smaller than those of GRC or OPC, and there were differences in the adhesive force within the fibers.

Figure 11 shows a scanning electron microscope (SEM) image of an ARG-added paste taken at 3000x magnification. The ARG-added paste underwent a curing process identical to the flexural strength specimens up to a material age of 28 d. It can be seen from the images that there are no signs of deterioration on the ARG surface in any of the specimens.

Figure 12 shows the fracture profile of a flexural strength specimen at a material age of 28 d, taken with an optical
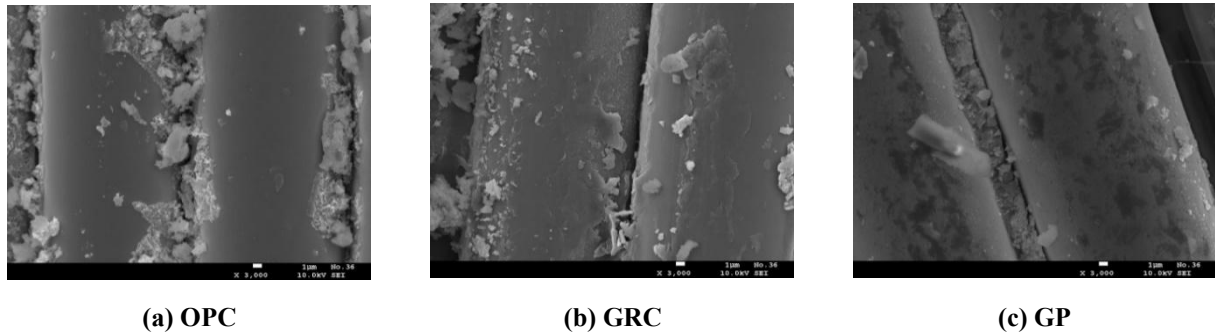
(a) OPC   (b) GRC   (c) GP

Figure 11. SEM image of ARG-added paste taken at 3000x magnification (Experiment 3)

(a) OPC   (b) GRC   (c) GP

Figure 12. Fracture profile of bent specimen at a material age of 28 days taken with optical microscope (Experiment 3)

microscope. It can be seen from the photograph that the ARG that slipped out of the specimen and the fractured ARG were mixed in all fracture profiles, regardless of the magnitude of the flexural strength. However, the proportion of slipping out to fracture is unclear.

The experimental results show that the flexural strength of GRGP was lesser flexural strength when compared with that of GRM, using OPC and GRC. However, there were no signs of ARG deterioration in GP during the initial material age period, when the material was placed in a high alkaline environment. Therefore, evaluating the progress of ARG deterioration over longer periods of material age is required. However, our results indicate that GRGP can be used as an exterior material for construction if the strength of the GP can be increased.

In future work, we plan to increase the strength of the GP mortar and evaluate its specimens, to also investigate the long-term deterioration of ARG.

4. Conclusions

The experimental results can be summarized as follows.

(1) The compression strength of the GP mortar tended to decrease with an increase in the ST addition rate regardless of AW/F, but the fluidity improved by adding ST at a rate of over 1.0%.

(2) Adding ARG did not influence the compression strength of GRGP.

(3) The flexural strength of GRGP was lesser than that of GRM using OPC and GRC. However, no alkali-induced ARG deterioration was observed at a material age of 28 d.

Acknowledgements

References

[1] S. Akihama, T. Suenaga, H. Nakagawa, H. Fujii (1986). MECHANICAL PROPERTIES AND DURABILITY OF GLASS FIBER REINFORCED CEMENT USING GRC CEMENT, Proceedings of the 8th Japan Concrete Institute Conference, pp. 417-420

[2] S. Goto, T. Inukai, Y. Uehara, and T. Hirose (2018). EFFECT OF SODIUM METASILICATE ADDITION METHOD AND SET RETARDING MIXTURES ON THE COMPRESSION STRENGTH CHARACTERISTICS AND FLOW VALUE OF A GEOPOLYMER OVER TIME, Proceedings of the Japan Concrete Institute, Vol. 40, No. 1, pp. 1821-1826

[3] S. Goto, T. Inukai, A. Maegawa, T. Hirose (2019), EFFECT OF GEOPOLYMER MIXING METHOD AND SIMULATED DRY SLUDGE POWER MIXING RATE ON THE COMPRESSION STRENGTH: Proceedings of the Japan Concrete Institute, Vol. 41, No. 1, pp. 1943-1948

[4] J. Davidovits. (2011). Geopolymer Chemistry and Applications, Institute GEOPOLYMER

[5] Dr. Mrs. S. A. Bhalchandr and Mrs. A. Y. Bhosle (2013). PROPERTIES OF GLASS FIBRE REINFORCED GEOPOLYMERCONCRETE, International Journal of Modern Engineering Research, Vol. 3, No. 4, pp. 2007-2010

[6] K. Korniejenko, J. Mikula and M. Lach (2015). CHARACTERIZATION OF MECHANICAL PROPERTIES OF SHORT GLASS FIBER-REINFORCED GEOPOLYMER COMPOSITES，10th International Conference on Composite Science and Technology

[7] Japan GRC Industrial Association (1998). GRC Industrial Association Standard, pp. 1-8, 55-57

[8] D. Hardjito and B. V. Ranga (2005) DEVELOPMENT and PROPERTIES OF LOW-CALCIUM FLY ASH-BASED GEOPOLYMER CONCRETE, Research Report GC 1 Faculty of Engineering Curtin University of Technology, Perth, Australia

[9] Japan GRC Industrial Association (1996). Physical Properties of GRC and Its Testing Methods, pp. 70-74

[10] Nippon Electric Glass Co., Ltd. (2000). Pre- Mixed GRC Technical Data (Basic Edition), pp. 2-4

[11] Kunihiro H., Hiroshi Y., Tadahiko S. and Takashi W. (1993). A STUDY ON HIGH FLUID PREMIXED GLASS-FIBER REINFORCED CONCRETE: Proceedings of the Japan Concrete Institute, Vol. 15, No. 1, pp. 963-968